Normal Stresses and Interface Displacement: Influence of Viscoelasticity on Enhanced Oil Recovery Efficiency

J. Avendano, Nicolas Pannacci, Benjamin Herzhaft, Patrick Gateau, Philippe Coussot

Oil & Gas Science and Technology – Rev. IFP Energies nouvelles

DOI: 10.2516/ogst/2012063

Dossier

Challenges and New Approaches in EOR
Défis et nouvelles approches en EOR

Normal Stresses and Interface Displacement: Influence of Viscoelasticity on Enhanced Oil Recovery Efficiency

J. Avendano[1]*, N. Pannacci[1], B. Herzhaft[1], P. Gateau[1] and P. Coussot[2]

1 IFP Energies nouvelles, 1-4 avenue de Bois-Préau, 92852 Rueil-Malmaison Cedex - France
2 Université Paris-Est, Institut Navier, IFSTTAR, 2 allée Kepler, 77420 Champs-sur-Marne - France
** Now with Universidad de los Andes, Laboratorio FIRP, Mérida, 05101 - Venezuela*
e-mail: avenbj@ula.ve - nicolas.pannacci@ifpen.fr - benjamin.herzhaft@ifpen.fr - patrick.gateau@ifpen.fr - philippe.coussot@ifsttar.fr

* Corresponding author

Résumé — Contraintes normales et déplacement d'interface : influence de la viscoélasticité sur l'efficacité de la récupération assistée — Une des méthodes de récupération assistée du pétrole (EOR - *Enhanced Oil Recovery*) consiste à injecter dans les puits des solutions aqueuses de polymère pour améliorer le rapport de mobilité entre le fluide injecté et le pétrole qui reste dans le puits. Ce procédé de "*polymer flooding*" est communément caractérisé par la seule valeur de la viscosité à faible gradient de vitesse du fluide injecté, bien que les solutions employées présentent une forte rhéofluidification et également de fortes propriétés élastiques mises en évidence par l'apparition de contraintes normales. Afin d'étudier les mécanismes mis en jeu au niveau de l'interface, nous avons développé des expériences modèles simples pour quantifier l'influence des propriétés viscoélastiques dans le cas d'un fluide déplaçant un autre dans une géométrie simple.

A cette fin, nous proposons et caractérisons un fluide modèle avec des composantes visqueuses et élastiques ajustables. Nous étudions ainsi le déplacement d'une huile visqueuse par un fluide Newtonien non élastique, un fluide viscoélastique ou un fluide purement rhéofluidifiant dans une cellule d'écoulement à deux dimensions. L'observation de la forme de l'interface entre la phase aqueuse et l'huile déplacée permet d'apprécier les effets de la viscoelasticité sur le déplacement. En utilisant une géométrie modèle et des fluides aux propriétés rhéologiques contrôlées, nous montrons que des fluides viscoélastiques ont tendance à mieux déplacer un fluide immiscible qu'un fluide Newtonien dans une cellule à deux dimensions et que ces effets sont liés à l'apparition de contraintes normales indépendamment des propriétés de rhéofluidification ou de variation de tension interfaciale dès que les effets visqueux dominent l'écoulement.

Abstract — Normal Stresses and Interface Displacement: Influence of Viscoelasticity on Enhanced Oil Recovery Efficiency — *One of chemical Enhanced Oil Recovery (EOR) methods consists in injecting aqueous solutions of polymers into the reservoir in order to improve mobility ratio between the injected fluid and the remaining oil. This "polymer flooding" process is usually only characterized with the low shear viscosity of the injected fluid, even if these aqueous solutions are strongly shear thinning and may show high elastic properties evidenced by normal stresses appearance. In order to study the mechanisms at the interface level, we develop simple model experimentations with the goal of quantifying the influence of viscoelastic properties on fluid displacement in a simple geometry.*

For this purpose, we propose and characterize a model fluid formulation, for which elastic and viscous effects can be tuned systematically. We study then the displacement of a viscous oil by a Newtonian non

elastic, a viscoelastic or a purely shear thinning fluid in a two dimensional flow cell. Observing the shape of the interface between aqueous fluids and displaced oil permits to appreciate viscoelasticity effects on the displacement. Using model geometries and controlled rheology fluids, we show that viscoelastic fluids tend to better displace immiscible liquids than Newtonian fluids and that those effects are closely related to the apparitions of normal stresses independently of shear thinning property or variation of interfacial tension as soon as viscous effects govern the flow.

INTRODUCTION

Chemical EOR (Enhanced Oil Recovery) processes consist in the injection of a chemical formulation into the reservoir that will promote the displacement of oil toward the producing well. Different formulations may be used depending on the reservoir characteristics and the technico-economical balance of the project.

Injection of polymer will enhance the recovery at a macroscopic scale by improving the mobility ratio between the oil and the displacing fluid, while surfactant or alkaline surfactant processes will mobilise residual oil at a microscopic scale by decreasing capillary forces that trap the oil into the reservoir. In polymer flooding, the trapping conditions (depending on the interfacial tension between oil and aqueous phase) will be quasi equivalent to a secondary recovery (water injection), therefore, the recovery efficiency at the microscopic scale is theoretically not modified [1].

The polymers commonly used in polymer flooding are synthetic polyacrylamides at concentrations ranging from 200 to 2 000 ppm, with high molecular weight – usually around 20×10^6 g/mol – and with various degree of hydrolysation [2]. Rheological behaviour of such polyacrylamide solutions shows two features that may be specially noticed. First, the fluid is extremely shear thinning and second, there is an elastic component which is not negligible under the form of the first normal stresses difference (N_1).

Non linear properties, such as normal stress differences and extensional viscosity, exist as a result of anisotropic microstructures (which is the case of polyacrylamides) and the ability to recover its structure when subjected to shear and extensional stress. Normal stresses are responsible of phenomena like Weissenberg effect (rod climbing) or "die swell" (post extrusion swelling of elastic fluids), in the other hand, extensional viscosity is defined as the resistance of the fluid to an extensional flow like one can encounter in flow in porous media [3].

Since the first studies on enhanced oil recovery, a very few fields did have implemented polymer flooding at a large scale. The Daqing field in China is one of the rare examples where tertiary recovery by polymer flooding has been heavily experienced since 1996. Additional recovery of oil around 11% was obtained [4]. With more than ten years of practicing polymer flooding, the Daqing field is an important source of information and is a proof of the effectiveness of this process. While the theoretical increase of oil production is usually attributed only to the mobility ratio improvement, some recent experimental observations from Daqing field, suggest that the viscoelasticity of polyacrylamide solutions (characterized by the first normal stress difference) contributes to improve the mobilization of residual oil at a microscopic scale [5]. Even if several mechanisms at the pore scales have been proposed to explain these observations, no clear distinction between viscous, extensional and elastic effects on oil mobilization and displacement has been established.

With the purpose of decoupling mechanisms and examining elastic influence at a relevant scale, we try in this work to establish the effect of the elastic property of a displacing fluid on the dynamic interface formed with an immiscible displaced fluid. To do so, we propose very simple experiments with model fluids that have been specially designed to tune independently elastic and viscous components.

The driving of a more viscous fluid by a less viscous one has been widely studied [6]. When viscous effects are sufficiently large compared to capillary effects that leads to the Saffman-Taylor instability, where the interface evolves in the form of fingers because this feature minimizes the viscous dissipation. For larger capillary effects a single finger finally forms through the viscous fluid. It was shown that a viscoelastic behaviour of the pushed fluid tends to increase this finger width [7]. This suggests that the opposite effect could occur if the non-viscoelastic fluid is pushed. The lack of studies of this configuration, less viscous fluids pushed by more viscous viscoelastic fluids, and its potential importance in polymer flooding establishes the motivation of our study.

1 BACKGROUND

Since the pioneering work of Stegemeier [8], it is well known that the oil saturation at the pore scale can be substantially decreased only if the capillary number (balance between viscous and capillary forces) is largely increased (at least two or three decades). Using polymer flood leads to a capillary number only several times higher than the waterflood value, therefore not enough to play a role on the microscopic scale oil displacement. However, since these early days, several experimental observations on cores and in the field showed higher recovery when using polymer flood than using waterflood [9]. The high recovery factor that has been attained in Daqing after several years of polymer flooding (up to 12% [5]) has led to attribute the increase in displacement efficiency to the viscoelastic nature of the injected polymer solutions. In 2000 [10], experiments on cores showed that the oil

recovery was 5 to 8% higher when polymer flooded than when water flooded. Similar results came from the field where the recovery for polymer or ASP (Alkaline Surfactant Polymer) processes was every time higher than excepted from theoretical curves taking into account only the capillary forces. Experiments on glass-etched cores gave the same results, and explanations were proposed regarding the elastic properties of the displacing fluids. Wang *et al*. [11] performed several experiments on cores and on micromodels with different pores configurations. In 2002 [5], they showed with experiments of microscopic percolating flow that visco-elasticity plays a role on the recovery for various types of residual oil (droplet, oil film, dead-end pore, etc.) and that residual oil could be pulled into an "oil thread channel" when using polyacrylamide solutions. In 2006, Yin *et al*. [12] proposed a numerical simulation of flowing of viscoelastic fluids in "dead-end pores" using a Modified Upper-Convected Maxwell rheological model (MUCM) taking into account elasticity and shear thinning properties of polyacrylamide solutions. The main conclusion was that the fluid viscoelasticity plays a major role in the improvement of recovery in dead-end pores, by enlarging flow lines therefore diminishing no flow zones. Several other publications from Daqing researchers confirm this effect, proposing qualitative mechanisms linking the effect of driving fluid elasticity to the modification of micro flow lines at the pore scale. Huh and Pope [9] performed a stability analysis of an oil column surrounded by a polymer annulus in a circular tube configuration. They showed that the elasticity of the polymer solution (represented by a Maxwell fluid model) could delay the breakage of the oil column into droplets, thereby reducing the oil saturation. More recently, Wang *et al*. [13] published field results showing that the use of viscoelastic fluid flooding yields very good results with incremental oil recovery about 20% of the original oil in place (almost twice the recovery obtained with conventional polymer flooding). They also claimed that the economics of the method as well as the technical difficulty linked to fluid management are about the same as a classical polymer flood.

All these innovative observations lead to the conclusion that the non-Newtonian characteristics of the displacing fluid in polymer flooding do play a role in the oil displacement at the pore scale. In order to describe the physical mechanisms that are at the origin of these effects, one needs to distinguish between the different non-Newtonian rheological properties that are significant for polymer fluids, and to establish quantitatively the effects on simple flow characteristics before gathering these mechanisms into a unified recovery model.

With this objective, we decided to focus on a sufficiently simple situation and to study the influence of elastic properties of a displacing fluid on the dynamic interface with a lower viscosity displaced fluid in a straight channel. In order to clarify the situation regarding the viscoelastic properties and in particular distinguish the impact of elastic and shear thinning effects, we worked with model fluids well characterised, with the ability to adjust normal stresses, and shear thinning property.

2 MATERIALS AND METHODS

2.1 Experimental Setup

As shown in Figure 1, our experimental set up consists in a rectangular cross section channel made of glass (thickness: $2d$ = 2 mm; width: D = 2 cm) partially filled with a viscous displacing fluid. Different types of displacing fluids are used: a Newtonian one, a viscoelastic one and a shear thinning one; they are detailed below. A less viscous Newtonian oil (Silicon oil HV100, *Rhodorsil*) of viscosity 0.1 Pa.s is introduced by the top of the cell.

At rest, without any flow, the interface between both fluids is slightly concave due to wetting of the aqueous phase on the hydrophilic glass surface. The channel is mostly filled with oil (top) and partly with the viscous displacing fluid (bottom). The interface is located at a distance from the lower inlet around five times the channel width, which is larger than the theoretical entrance length (l_e) [14]. Entrance effects are then expected to be negligible on the subsequent flow characteristics around the interface.

The displacement experiment begins with the injection, at constant flow rate Q, of the viscous displacing fluid from the lower inlet using a syringe pump system, that pushes the oil vertically through the channel with an injection velocity of magnitude v ($v = Q/2dD$). Flow characteristics are observed from that time following the evolution of the interface from above the largest channel side (plane (x,y) in which x is the main flow direction). Images are acquired with a CCD camera (50 Hz) and processed with MATLAB in order to obtain the

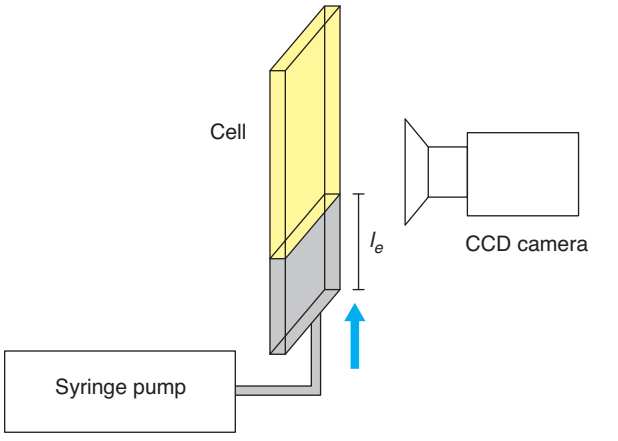

Figure 1

Experimental setup.

interface profiles. All the displacements experiments into the channel and rheological tests were carried out at room temperature (22 ± 1°C). The Reynolds numbers range covered by these experiences is between 1×10^{-2} and 10.

Within the displacement experience, two periods can be differentiated. The first one represents a non-steady state in which the shape of the interface continuously evolves until a definitive shape is reached, representing the beginning of the steady state zone. This final, stabilised shape can thus be considered characteristic of a given flow condition.

2.2 Formulation and Characterization of Fluids

As for the Newtonian displacing fluid, we used a sugarcane syrup (*Canadou*©) with a constant viscosity $\eta = 0.16$ Pa.s, considered as the reference Newtonian fluid. The viscoelastic system is a non-hydrolyzed PAM (Polyacrylamide, *Aldrich*) in a water-Canadou solution as solvent and NaCl (0.2%) to impose a constant ionic strength. This system was chosen for two main reasons: its viscosity is nearly constant in a wide range of shear rates and it exhibits elastics properties which can be modified through formulation. Such a fluid is derived from the viscoelastic fluids known as Boger fluids [15-18]. Two viscoelastics formulations with different elastic levels, as a result of different concentrations of the same polymer (6 000 and 4 000 ppm of Polyacrylamide in water, 0.2% NaCl) were formulated. They are respectively named in the following PAM-6000 and PAM-4000. We also used a water-Xanthan (5 000 ppm of Xanthan, *Aldrich*) solution which represents a non-elastic shear thinning fluid.

The rheological characteristics of these fluids in steady state simple shear, *i.e.* the shear stress τ and the first normal stress difference N_1 as a function of the shear rate $\dot{\gamma}$, were measured with a controlled stress rheometer (AR2000, *TA Instruments*) equipped with a cone and plate geometry (diameter: 4 cm; angle: 2°). The normal force was measured *via* a gauge placed below the bottom plate. In addition, we have performed oscillatory tests in order to determinate the relaxation time (λ) of the viscoelastic formulations using the same geometry. Note that in such a geometry, in a spherical coordinate system (θ, ϕ, t) with θ the angle from the vertical central axis and r the distance from the central point, we have $\dot{\gamma} = (\sin\theta) dv_\phi/d\theta$, $\tau = \sigma_{\theta\phi}$ and $N_1 = \sigma_{\theta\theta} - \sigma_{\phi\phi}$, where v_ϕ is the azimuthal velocity and $\sigma_{ij \in \theta, \phi, r}$ are the stress tensor components [19]. Rheological characterizations are shown in Figure 2 and Figure 3.

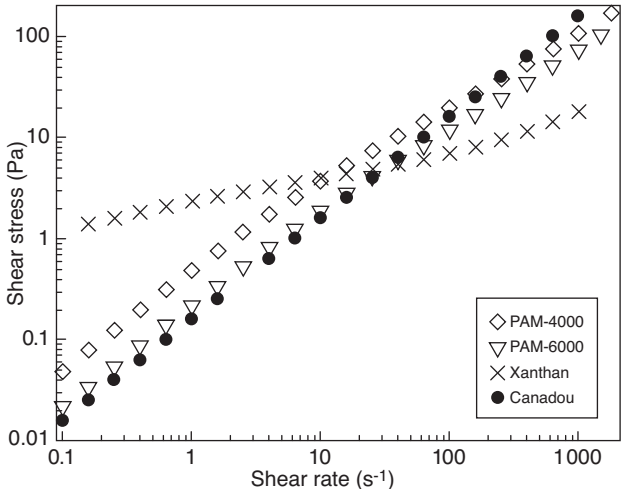

Figure 2

Stress-shear rate curves of displacing fluids: Newtonian Canadou (●), viscoelastic PAM-4000 (◇), PAM-6000 (▽) and shear thinning Xanthan solution (×).

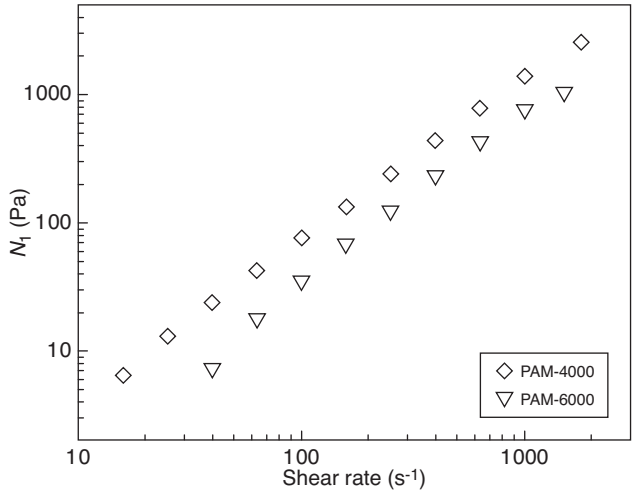

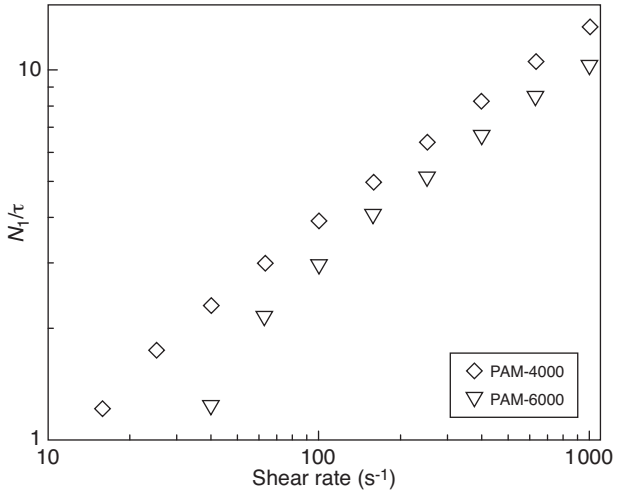

Figure 3

N_1 as a function of shear rate for PAM-4000 (◇) and PAM-6000 (▽), on the right N_1/τ is shown for PAM-4000 (◇) and PAM-6000 (▽) as a measure of its elasticity.

The two viscoelastic systems and the Newtonian fluid exhibit shear viscosities larger than the oil viscosity and roughly similar in the range between 1 and 1000 s^{-1}.

The data for normal stress difference were reproducible and reliable only above a threshold value of the order of 10 Pa. For the Xanthan solution N_1 was insignificant. It is remarkable that for the PAM solutions N_1/τ progressively increases from about 0.5 to 10 when $\dot{\gamma}$ increases from 10 s^{-1} to 1 000 s^{-1}. The more concentrated solution of PAM is considered to be more "elastic" because its relative normal force (N_1/τ) is greater compared to the less concentrated solution. As additional information, normal forces begin to be relevant (more than 10 Pa) in PAM-6000 for shear rate around 30 s^{-1} and above; on the other side, the same is true for PAM-4000 for shear rate around 70 s^{-1}.

The interfacial tension between the viscous fluids and the oil was measured with a tensiometer (TK100, *Kruss*) and was between 26.1 ± 0.5 mN/m and 34.5 ± 0.3 mN/m. For some tests, we obtained a much lower value (ten times lower than the non-treated interface) by adding a surfactant SPAN80 (1%) to the silicon oil.

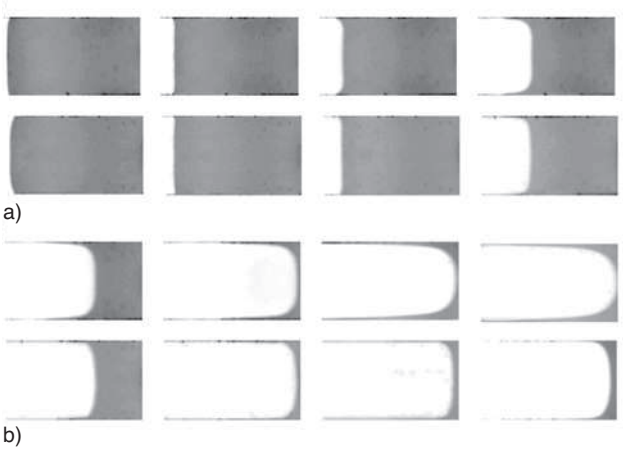

Figure 4

Successive views of the interface profile in the plane (x, z) for the Newtonian fluid (upper pictures) and PAM-6000 (lower pictures) at different times for injection velocity of 10 cm/s: a) 0 s, 0.3 s , 0.5 s, 0.6 s; b) 0.8 s, 1 s, 1.5 s and 2 s. Note that the first six pictures correspond to 0 cm < x < 5 cm while the two last ones (on the right of b)) respectively correspond to 5 cm < x < 10 cm and 10 cm < x < 15 cm.

3 RESULTS AND DISCUSSIONS

3.1 Imposed Flow Rate Displacement Experiment: Newtonian *vs* Elastic

The first oil displacement experiments *(Fig. 4)* were carried out at imposed flow rates for both the Newtonian and the most elastic fluid (PAM-6000) and the following observations were established:

– the oil/fluid interface is displaced in both cases at the same macroscopic velocity (as expected, because it's a consequence of the constant imposed flow rate);
– the shape of the interface reaches a steady-state after certain distance inside the cell;
– that shape is well distinguishable when the Newtonian and the elastic fluid are compared.

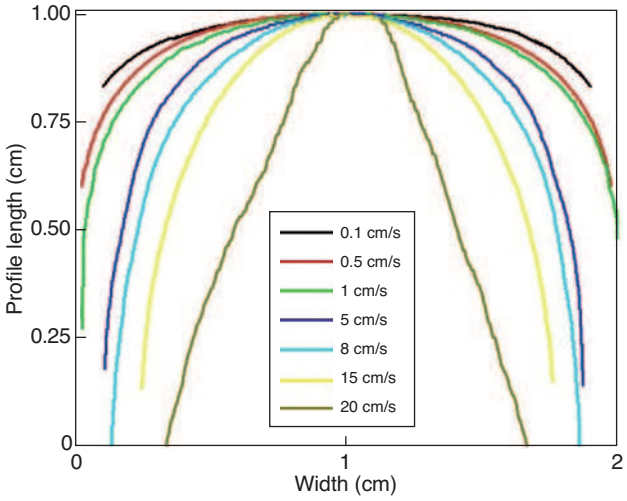

Figure 5

Profiles of the Newtonian fluid/silicone oil interface between 0.1 cm/s and 20 cm/s. Higher velocities lead to a reduction of the Newtonian fluid penetration into the oil.

3.2 Influence of the Flow Rate on the Steady State Profile: Newtonian *vs* Elastic

A further study varying the imposed flow rate shows that for the Newtonian displaced fluid, the shape of the steady state interface depends on the velocity of the displacing fluid. The interface is sharper as the velocity of the displacing fluid increases.

To explain what is seen in Figure 5, we consider that the interfacial tension acts like a stabilizing element of the profile whereas the injection velocity of the fluid, representative of its inertia, has the role of destabilizing effect [20]. In these experiments, interfacial tension is constant, and a progressive increase of the volumetric flow results in the total instability of the interface front, which indeed occurred when the front velocity was higher than 20 cm/s (where the Reynolds number is approximately 5). A Newtonian fluid displacing oil of lower viscosity will diminish the displacement efficiency in this geometry as its velocity increases.

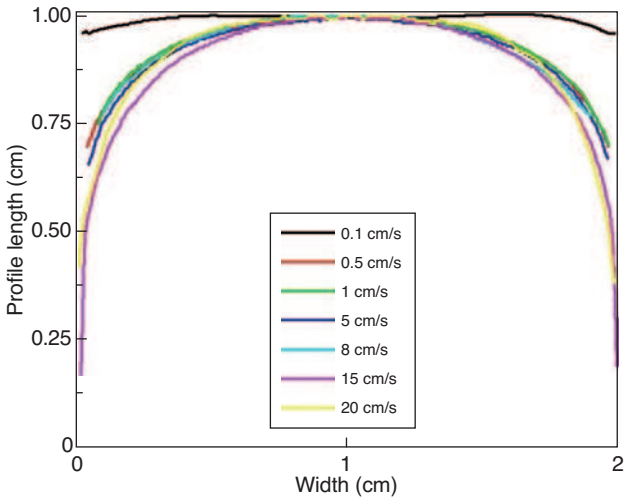

Figure 6

Profiles of PAM-6000 between 0.1 cm/s and 20 cm/s. With exception of very low velocity, penetration of PAM-6000 into the oil is constant within a long range of velocities.

We performed then similar experiments using the viscoelastic fluid (PAM-6000) as a displacing fluid. The interface profiles are shown in Figure 6. It shows that the shape of the interface is in this case, essentially independent of the displacing fluid velocity, with the exception of very low velocities where interfacial tension may play a substantial role.

We can point-out that under the same inertial conditions and with a similar surface tension, the interface profiles of the Newtonian fluid – oil system, are very different compared to the PAM-6000 – oil case. The only additional factor that we can consider to explain these differences is the elasticity of the formulations.

This observation is in agreement with Lee's observations [21, 22], who studied the displacement of Newtonian and viscoelastic fluids with air. Their experiments show that the shape of the interface changes according to the fluids and their elasticity level. One of the basic conclusions is that the elasticity of the fluid seems to retain the deformation originated by the air.

3.3 Quantifying the Difference between Steady State Profiles: Newtonian *vs* Elastic Fluids

We propose a macroscopic criterion to quantify this effect, named the additional displaced oil (φ). It represents the ratio between the apparent surface of oil displaced by a fluid and the apparent surface of oil that is displaced for a Newtonian fluid under the same flow conditions. If this value is positive the studied fluid is more effective for the displacement of oil than the Newtonian fluid:

$$\varphi = \frac{Surface\ displaced\big|_{VE\ fluid} - Surface\ displaced\big|_{Newtonian\ fluid}}{Surface\ displaced\big|_{Newtonian\ fluid}}$$

In the following, we compare the evolution of this parameter calculated for a 1 cm long profile in the *x*-direction, as a function of the flow characteristics. These flow characteristics will be expressed through the values of dimensionless numbers which represents the ratio of typical forces in the experience: the capillary number *Ca* ($Ca = \eta v/\sigma$, where σ is water-oil interfacial tension) which represents the relation between viscous forces and interface forces, and the Weissenberg number *Wi* ($Wi = \lambda\dot{\gamma}$) as a measure of the elasticity of the fluid. The results can be seen in Table 1.

TABLE 1

Parameter φ for PAM-6000 is shown for different flow conditions. *Ca* number is similar when compared to the Newtonian fluid, meanwhile φ increases as *Wi* is higher

Velocity (cm/s)		PAM-6000			Newtonian fluid	
	φ	*Ca*	*Re*	*Wi*	*Ca*	*Re*
0.5	0.01	0.046	0.07	0.582	0.023	0.15
1	0.03	0.083	0.16	1.164	0.046	0.3
5	0.23	0.292	1.31	5.821	0.229	1.48
8	0.41	0.419	2.36	9.314	0.366	2.36
15	1.11	0.677	5.9	17.46	0.686	4.43

As we can see, for 0.5 cm/s and 1 cm/s the interface shape is very similar, with these conditions interface forces are dominant. When differences become relevant interface forces have decreased (as a consequence of viscous forces augmentation) and inertial forces have increased but this is happening in both fluids. The only substantial difference that we can see is evidenced in *Wi*, which actually goes from 0.58 to 17.5 in that velocity range. This analysis confirms that interfacial tension tends to stabilize the interface formation at very low velocities but is not that effective at high velocities, where elasticity tends to establish the shape of the interface.

In order to drastically change one of the parameters, low interfacial tension experiences were carried out. We add a surfactant to the displaced fluid in order to lower the interface tension by a decade and then obtained a capillary number ten times higher. Those results are gathered in Table 2.

With these results, at low velocities we still have a dominance of interface forces, but when elastic forces begin to be relevant, interface shape is rapidly affected. On the other hand, as interfacial tension was 10 times decreased, interface stability is affected in general as expected in [23]. As a consequence, φ remains lower compared to normal tension experiences.

TABLE 2

Parameter φ for PAM-6000 in low tension experiences

Velocity (cm/s)		PAM-6000			Newtonian fluid	
	φ	*Ca*	*Re*	*Wi*	*Ca*	*Re*
0.5	0	0.429	0.07	0.582	0.256	0.15
1	0.004	0.774	0.16	1.164	0.512	0.3
5	0.04	2.721	1.31	5.821	2.549	1.48
8	0.18	3.905	2.36	9.314	4.074	2.36

3.4 Normal Stress Difference as a Measure of Elastic Effects on Interface Shape

Nevertheless, the term elasticity needs to be precised. In our experiments in the uniform channel, the flow develops mainly along a single direction so that the extensional flow contribution is generally much smaller than the shear flow contribution. The flow characteristics are more complex around the interface as a result of the slight motion of recirculation of the fluid which makes it possible to keep a stationary interface while the velocity is certainly not uniform in each fluid region. However, this motion does not specifically involve an extensional flow, it is essentially a simple shear in a rotating frame. At last, there is also some extensional flow component due to the entrance in the channel but in our case the interface at the beginning of the test was situated sufficiently far from the entrance. Finally, the extensional components in the strain rate tensor can be considered as negligible, which implies that in our tests extensional effects were negligible regarding the effects of normal stress difference.

Considering this feature, we are going to state that N_1 is a good measure to reflect the appearance of the elastic effects in this geometry. In Figure 7, profiles of PAM-4000 are compared against the Newtonian fluid at 1 cm/s and no difference between those profiles is found; velocity of the displacing fluid has to be raised to 5 cm/s for differences between those profiles to begin to manifest. In Figure 8, the same fact is verified when the profiles of PAM-6000 are compared against the Newtonian fluid, but in this case, at 1 cm/s the profiles are already different, it is necessary to descend to very low velocities as 0.5 cm/s to have similar profiles between the Newtonian and the viscoleastic fluid.

Considering that the front velocity of 1 cm/s corresponds to a shear rate of 30 s^{-1} (calculated as the average shear rate in the geometry) the difference between PAM-6000 and PAM-4000 lies in the existence of non-negligible N_1 value. For PAM-6000 N_1 value is about 40 Pa at 30 s^{-1} (corresponding to a 1 cm/s velocity) whereas for PAM-4000, it is negligible with these shear conditions. To corroborate this observation, when the front velocity is 0.5 cm/s, the corresponding shear rate (average shear in the geometry) is 15 s^{-1}, N_1 value is just above 10 Pa for the PAM-6000, which is fairly low and therefore considered negligible and not enough to be relevant to affect the profile. Saying this, we propose that the origin of the differences between the profiles is related to the magnitude of displacing fluid normal stress difference N_1.

Moreover, Figure 6 indicates that these normal stress effects, as soon as they start to be significant, tend to stabilize the profile to a given general shape, with no evolution when normal stress continues to rise. This surprising result suggests that when elastic component is increased, some additional

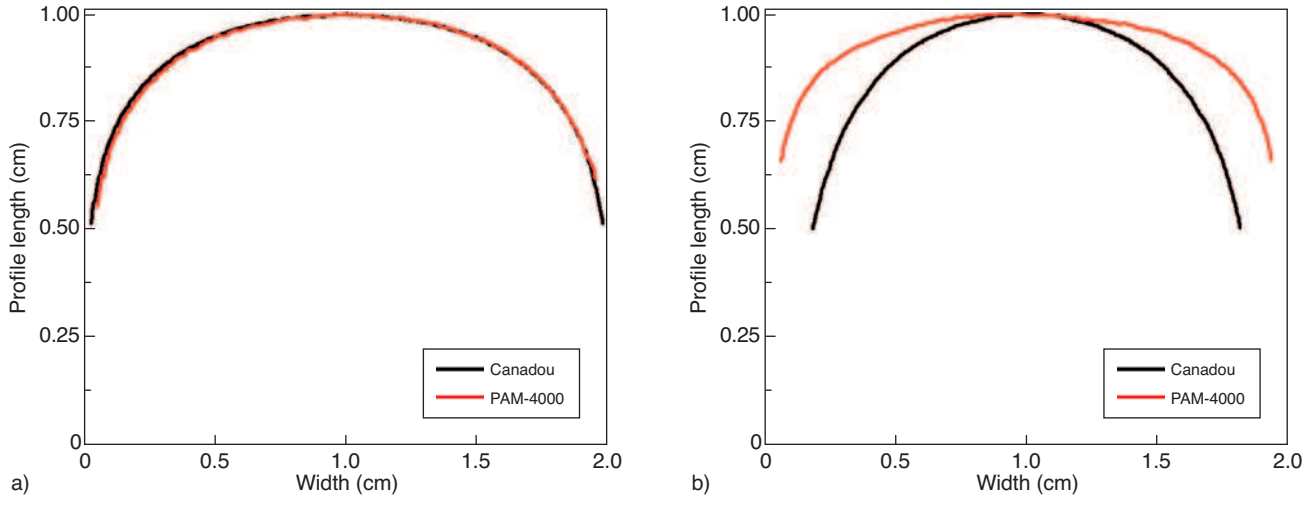

Figure 7

Comparison of interface profiles between PAM-4000 and the Newtonian fluid a) at 1 cm/s no difference is noticed, b) at 5 cm/s, profiles are completely differentiated.

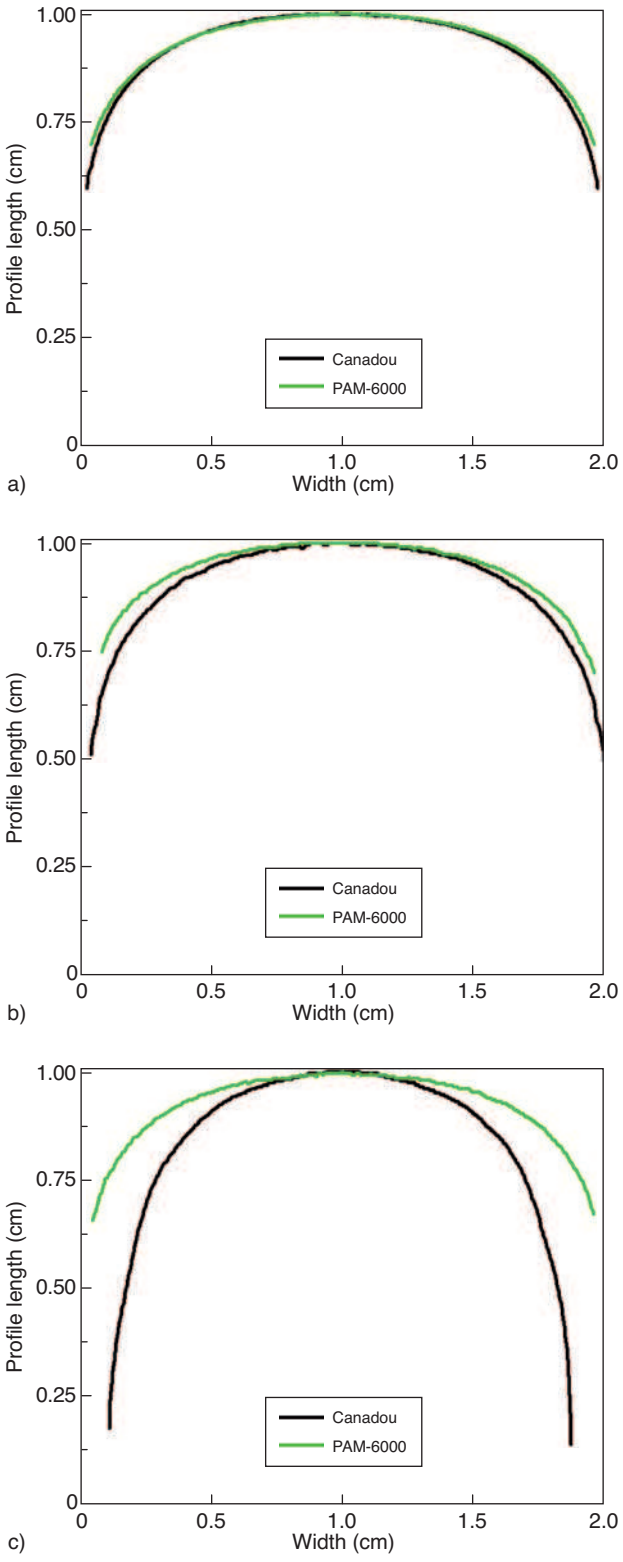

Figure 8

Comparison of interface profiles between PAM-6000 and the Newtonian fluid. a) At 0.5 cm/s, no difference is noticed. b) At 1 cm/s, profiles starts to be differentiated. c) Finally, at 5 cm/s, the viscoelastic profile is much more flat compared to the other.

effect linked to interfacial, viscous and inertial forces tends to damp the interface deformation resulting in the same equilibrium interfacial shape. Further study with fluids with even more precisely controlled rheological properties would be needed to get more information on that point.

3.5 Effect of the Shear Thinning Behavior in Steady State

Other experiments were conducted using no elastic shear thinning water-Xanthan formulation ($N_1 = 0$ for every shear rate) to push the oil. No difference can be seen when comparing the resulting interface shapes with those obtained with the Newtonian displacing fluid *(Fig. 9)* in a large range of velocities

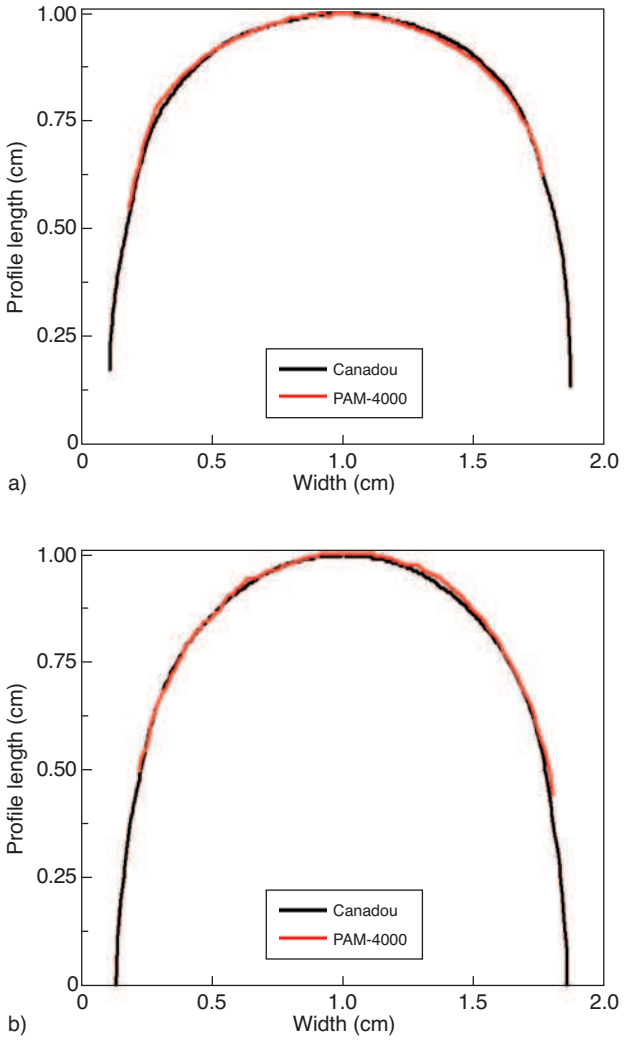

Figure 9

Comparison of interface profiles between Xanthan and the Newtonian fluid at a) 5 cm/s, b) 8 cm/s. No difference is noticeable between profiles

(and thus shear rates). This result shows that elasticity of the displacing fluid characterised by its normal stress, is responsible for the difference in the interface profile that have been demonstrated, whereas shear thinning property of the displacing fluid does not have any impact.

3.6 Normal Stress Impacts on Liquid-Liquid Interface Shaping: A Simple Model

A simple model provides a qualitative explanation to these effects. At equilibrium, the two fluids are simply behind each other in the channel. If surface tension and inertia effects are negligible during the start up flow phase, the flow characteristics in each fluid may be well described, as a first approximate, by those of the fluid as if it was alone in the channel. In a plane (x,y) far from the channel sides, at first order the velocity is independent of z and the only non-zero component (v) of the velocity is along the x axis. Locally, we thus have essentially a simple shear with a shear rate $\dot{\gamma} = dv/dy$. Under these conditions it may be shown that the stress tensor only depends on $\dot{\gamma}$, and the momentum equation reduces to $\partial\tau_{xy}/\partial y - \partial p/\partial x = 0$; $\partial\tau_{yy}/\partial y - \partial p/\partial y = 0$, in which p is the pressure and τ_{xy} and τ_{yy} are the shear and normal stresses. In the (Newtonian) oil, we have $\tau_{xy} = \eta\dot{\gamma}$ and $\tau_{yy} = 0$ and the momentum equation leads to $\partial\tau_{xy}/\partial y = A = \partial p/\partial x$, in which $A < 0$ is a constant. We deduce the usual "Poiseuille" velocity profile:

$$v(y) = -(A/2\eta)(d^2 - y^2)$$

For the sake of simplicity, we represent the steady state simple shear behaviour of our viscoelastic fluids with linear expressions for the shear and normal stresses: $\tau_{xy} = \eta\dot{\gamma}$, $\tau_{yy} = \alpha\dot{\gamma}$, in which α is a viscosity coefficient for the normal stress. This model is a rough approximation in the case of the PAM fluids for which one would need to assume η and α to be apparent viscosities varying with $\dot{\gamma}$. Since τ_{yy} only depends on y, the momentum equation implies that the pressure expresses as $p = f(y) + g(x)$.

As this pressure gradient is maximum at the center of the cell and propagates in all directions, a constant value is finally deduced: $g(x) + Ax$ with $\partial\tau_{xy}/\partial y = A$, so that the velocity profile is still given by the above Poiseuille law. However the pressure is now given as $p(x, y) = Ax + \alpha\dot{\gamma} = A(x + \alpha y/\eta)$, in which the additional integration constant was dropped.

Thus when the fluid developing normal stresses is alone in the channel, its flow characteristics are similar to those of a simple Newtonian fluid except that the pressure distribution is more complex. When it is in contact with a Newtonian fluid for which the pressure simply varies linearly with x the interface does not simply result from the fluid deformation according to Poiseuille law, since it would not allow for the pressure continuity (expected in the absence of surface tension effects). The interface shape will tend to adjust in order to take into account the pressure shift due to the normal stress

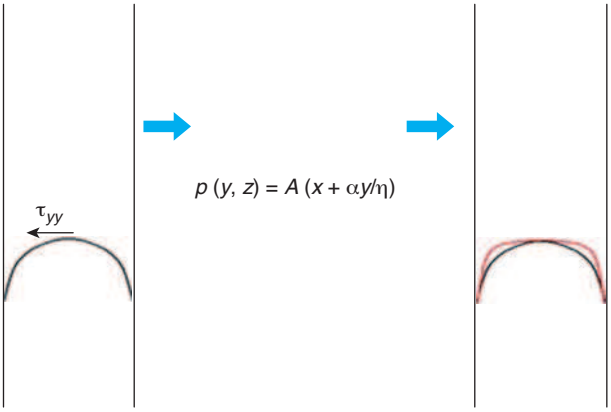

Figure 10

An overpressure approach is proposed to explain the effect of elastic properties on the aqueous-oil interface profile in displacement experiments.

effect: according to the above equation, the interface will be shifted towards larger x (where the pressure is smaller) for larger y *(Fig. 10)*.

This approach is based on a few reasonable hypothesis and is in accordance with the trends observed in our data, even if it doesn't allow to deduce quantitatively the deformation of the resulting interface.

CONCLUSIONS

Using model geometries and controlled rheology fluids, we have shown that pushing a Newtonian oil by an immiscible fluid in an Hele Shaw cell is more efficient with viscoelastic fluids than with Newtonian fluids and that those effects are closely related to the apparitions of normal stresses independently of shear thinning property or variation of interfacial tension as soon as viscous effects govern the flow. This effect, that for the best of our knowledge has never been demonstrated, suggests that this property of viscoelastic fluids could be adjusted in order to optimize the efficiency in enhanced oil recovery. However for flow through more complex geometries such as porous media it remains, among others, to study whether the extensional effects do play a role. This study is under progress in order to progressively establish physical mechanisms that will provide a global understanding of viscoelastic influence on enhanced oil recovery.

REFERENCES

1 Nouri H.H., Root P.J. (1971) A Study of Polymer Solution Rheology, Flow Behavior, and Oil Displacement Processes, *Fall Meeting of the Society of Petroleum Engineers of AIME*, New Orleans, Louisiana, 3-6 Oct., *SPE Paper* 3523.

2 Terry R.E. (2000) Enhanced oil recovery, in *Encyclopedia of Physical Science and Technology*, 3rd edition, Vol. 18, Robert A. Meyers (ed.), Academic Press, pp. 503-518.

3 Barnes H. (2000) *A Handbook of elementary rheology*, The University of Wales (ed.), Dyfed.

4 Yupu W., He L. (2006) *SPE Asia Pacific Oil & Gas Conference and Exhibition*, Adelaide, Australia, 11-13 Sept.

5 Wang Demin, Sun Yingjie, Wang Yan, Tang Xuping (2002) Producing More Than 75% of Daqing Oil Field's Production by IOR, What Experiences Have Been Learnt? *SPE Asia Pacific Oil and Gas Conference and Exhibition*, Melbourne, Australia 8-10 Oct., *SPE Paper* 77871.

6 Saffman P.G., Taylor G. (1958) The Penetration of a Fluid into a Porous Medium or Hele-Shaw Cell Containing a More Viscous Liquid, *Proc. R. Soc. Lond. Ser. A* **245**, 1242, 312-329, doi: 10.1098/rspa.1958.0085.

7 Lindner A. (2000) L'instabilité de Saffman-Taylor dans les fluides complexes : relation entre les propriétés rhéologiques et la formation de motifs, *Thèse*, Université Paris 6.

8 Stegemeier G. (1977) Mechanisms of entrapment and mobilization of oil in porous media, in *Improved Oil Recovery by Surfactant and Polymer Flooding*, Shah and Schechter Academic Press, New York.

9 Chun Huh, G.A. Pope (2008) Residual Oil Saturation from Polymer Floods: Laboratory Measurements and Theoretical Interpretation, *SPE/DOE Symposium on Improved Oil Recovery*, Tulsa, Oklahoma, 20-23 April, *SPE Paper* 113417.

10 Wang Demin, Cheng Jiecheng, Yang Qingyan, Gong Wenchao, Li Qun, Chen Fuming (2000) Viscous-Elastic Polymer Can Increase Microscale Displacement Efficiency in Cores, *SPE Annual Technical Conference and Exhibition*, Dallas, Texas, 1-4 Oct., *SPE Paper* 63227.

11 Xia Huifen, Wang Demin, Wenxiang Wu, Haifeng Jiang (2007) *Asia Pacific Oil and Gas Conference and Exhibition*, [Wu Wenxiang, Wang Demin, Jiang Haifeng (2007) Effect of the Visco-elasticity of Displacing Fluids on the Relationship of Capillary Number and Displacement Efficiency in Weak Oil-Wet Cores, *Asia Pacific Oil and Gas Conference and Exhibition*, Jakarta, Indonesia, 30 Oct.-1 Nov., *SPE Paper* 109228].

12 Hongjun Yin, Wang Demin, Huiying Zhong (2006) Study on Flow Behavoirs of Viscoelastic Polymer Solution in Micropore With Dead End, *SPE Annual Technical Conference and Exhibition*, San Antonio, Texas, 24-27 Sept., *SPE Paper* 101950.

13 Wang Demin, Wang Gang, Xia Huifen (2011) Large Scale High Visco-Elastic Fluid Flooding in the Field Achieves High Recoveries, *SPE Enhanced Oil Recovery Conference*, Kuala Lumpur, Malaysia, 19-21 July, *SPE Paper* 144294.

14 Guyon E., Hulin J.P., Petit L. (2001) *Hydrodynamique physique*, EDP Sciences (éd.), Paris.

15 Boger D.V. (1977) A highly elastic constant-viscosity fluid, *J. Non-Newton. Fluid Mech.* **3**, 1, 87-91.

16 Binnington R.J., Boger D.V. (1986) Remarks on non-shear thinning elastic fluids, *Polym. Eng. Sci.* **26**, 2, 133-138.

17 Tam K.C., Moussa T., Tiu C. (1989) Ideal elastic fluids of different viscosity and elasticity levels, *Rheol. Acta* **28**, 2, 112-120.

18 Stokes J.R., Graham J.W., Lawson N.J., Boger D.V. (2001) Swirling flow of viscoelastic fluids. Part 2. Elastic effects, *J. Fluid Mech.* **429**, 117-153.

19 Markovitz H. (1980) The normal stress effect in polymer solutions, in *Mechanical and thermophysical properties of polymer liquid crystals*, Springer.

20 Hou T.Y., Li Z.L., Osher S., Zhao H.K. (1997) A hybrid method for moving interface problems with application to the Hele-Shaw flow, *J. Comput. Phys.* **134**, 2, 236-252.

21 Lee A.G., Shaqfeh E.S.G., Khomami B. (2005) Viscoelastic effects on interfacial dynamics in air-liquid displacement under gravity stabilization, *J. Fluid Mech.* **531**, 59-83.

22 Lee A.G., Shaqfeh E.S.G., Khomami B. (2002) A study of viscoelastic free surface flows by the finite element method: Hele-Shaw and slot coating flows, *J. Non-Newton. Fluid Mech.* **108**, 1-3, 327-362.

23 Hornof V. (1987) Gravity Effects in the Displacement of Oil by Surfactant Solutions, *SPE Res. Eng.* **2**, 4, 627-633, 11. *SPE paper* 13573.

Final manuscript received in August 2012
Published online in January 2013